

typical simulation run. The numerical curve starts with the inclination corresponding to the initial Maxwellian, but soon becomes practically identical with the theoretical asymptotic solution.

To summarize, the numerical simulations verify the main points of the theory: the prediction for the rotation of the spectrum with respect to the drift velocity, and the description of the electron diffusion by the unmagnetized quasilinear diffusion tensor, even for rather high levels of ion-sound turbulence. The results represent a direct verification of orbit perturbation theory first introduced by Dupree. The theory is easily extended to the three-dimensional case and the basic conclusions still hold. Details of the theory will be published in a forthcoming paper.¹⁰

*This work was performed under the terms of the agreement on association between the Max-Planck-Institut für Plasmaphysik and EURATOM.

¹M. D. Machalek and P. Nielsen, Phys. Rev. Lett. **31**,

439 (1973).

²K. Muraoka, E. L. Murray, J. W. M. Paul, and D. D. R. Summers, J. Plasma Phys. **10**, 135 (1973).

³A. D. Craig, S. Nakai, D. D. R. Summers, and J. W. M. Paul, Phys. Rev. Lett. **32**, 975 (1974).

⁴D. Biskamp and R. Chodura, Phys. Fluids **16**, 893 (1973).

⁵D. Biskamp, R. Chodura, and C. Dum, in *Proceedings of the Sixth European Conference on Controlled Fusion and Plasma Physics, Moscow, U.S.S.R., 1973*, (U.S.S.R. Academy of Sciences, Moscow, 1973), p. 461.

⁶C. Dum, R. Chodura, and D. Biskamp, Phys. Rev. Lett. **32**, 1231 (1974).

⁷C. T. Dum and T. H. Dupree, Phys. Fluids **13**, 2064 (1970).

⁸C. T. Dum and R. N. Sudan, Phys. Rev. Lett. **23**, 1149 (1969).

⁹M. Lampe, W. M. Manheimer, J. B. McBride, J. H. Orens, R. Shanny, and R. N. Sudan, Phys. Rev. Lett. **26**, 1221 (1971).

¹⁰C. T. Dum, to be published.

¹¹L. Spitzer, *Physics of Fully Ionized Gases* (Interscience, New York, 1962), p. 134.

¹²R. Z. Sagdeev and A. A. Galeev, International Centre for Theoretical Physics Report No. IC/66/64, 1966 (unpublished).

Surface-Wave Absorption*

J. M. Kindel, K. Lee, and E. L. Lindman

University of California Los Alamos Scientific Laboratory, Los Alamos, New Mexico 87544

(Received 24 June 1974)

The 50% peak absorption predicted for resonant absorption in a linear density profile can be raised to above 90% if a different profile is used which involves a sharp jump in density along which a surface wave may propagate. Collisionless-plasma simulation studies show that at high intensities the energy goes into fast electrons which are accelerated back out of the plasma into the vacuum.

Many studies of resonant absorption have been carried out which indicate that no more than 50% of the incident electromagnetic energy can be absorbed.¹⁻³ In these studies the plasma density was assumed to vary linearly as a function of position. When this assumption is relaxed a class of density profiles can be found in which a much larger percentage absorption can occur (~90% and higher). These profiles are characterized by the occurrence of a sharp jump in the density along which a surface wave⁴⁻⁵ may propagate. The generation of such profiles by the ponderomotive force in a plasma rarefaction, leading to more than 50% absorption over long periods of time, has been observed in plasma simulation studies.⁶ Whether or not a profile which gives 90% or more absorption occurs in any given experiment can be determined only by further studies of profile modification currently in progress.

Consider a plasma whose density is a function of x only. Incident on it is an electromagnetic wave with its propagation vector \vec{k} and its electric field vector \vec{E} in the x - y plane and its magnetic field vector \vec{B} in the z direction only. Neglecting the high-frequency ion motion, the linearized equations are

$$c \nabla \times \vec{E}_1 = \dot{\vec{B}}_1, \quad c \nabla \times \vec{B}_1 = \dot{\vec{E}}_1 - 4\pi n_{e0} e \vec{V}_{e1},$$

$$m(\dot{\vec{V}}_{e1} + \nu \vec{V}_{e1}) = -e \vec{E}_1 - (T_e/n_{e0}^2)[\gamma n_{e0} \nabla n_{e1} - n_{e1} \nabla n_{e0}] \dot{n}_{e1} + \nabla \cdot (n_{e0} \vec{V}_{e1}), \quad n_{e0} = n_0(x).$$

Assuming that all first-order quantities vary as $\exp(ik_y y - i\omega t)$, we obtain the following equations for $n = n_{e1}$ and $B = B_{z1}$ which characterize the system:

$$\epsilon \frac{d}{dx} \left(\frac{1}{\epsilon} \frac{dB}{dx} \right) + \left(\epsilon \frac{\omega^2}{c^2} - k_y^2 \right) B + \frac{k_y \omega_p^2 T_e}{\omega c} \frac{\omega + i\nu}{n_{0e}} \left[\frac{n_0'}{n_0} - \gamma \frac{\epsilon'}{\epsilon} \right] n_1 - \frac{k_y \omega_p^2 \gamma T_e}{\omega c} \frac{n_1}{n_0} \frac{d}{dx} \left(\frac{\omega + i\nu}{\omega + i\nu_L} \right) = 0, \quad (1)$$

$$\epsilon \frac{T_e}{Me} \frac{d}{dx} \frac{1}{\epsilon(\omega + i\nu_L)} \left[\left(\gamma \frac{dn_1}{dx} - n_1 \frac{n_0'}{n_0} \right) \right] + \omega \left[\epsilon - \frac{k_y^2}{\omega(\omega + i\nu_L)} \frac{\gamma T_e}{Me} \right] n_1 - \frac{e}{m_e} \frac{ck_y}{\omega} \epsilon \left[\frac{d}{dx} \left(\frac{n_0}{\epsilon} \frac{1}{\omega + i\nu} \right) \right] B = 0, \quad (2)$$

where

$$\omega_p^2(x) = 4\pi n_0(x) e^2 / m_e,$$

$$\epsilon(x) = 1 - \omega_p^2(x) / \omega(\omega + i\nu),$$

and primes indicate differentiation with respect to x . The phenomenological damping factor ν_L is included to describe approximately the effects of Landau damping and particle trapping which affect only longitudinal plasma waves. The absorption calculated from these equations is insensitive to the value of ν_L provided it is strong enough to damp plasma waves sufficiently to prevent their reflection from boundaries.

It is instructive to isolate the surface wave and establish some of its properties in the limit $T_e \rightarrow 0$. To this end, neglect the incoming light wave and consider a plasma which fills all space. For $x < 0$ it has a constant density such that $\omega_p = \omega_{p1}$, and for $x > 0$ a different constant density such that $\omega_p = \omega_{p2}$. The equation for B can then be solved trivially in each of the two regions. In order for a surface wave to exist, the solutions for B must be evanescent in both regions. Applying boundary conditions at infinity, one obtains

$$B(x) = \begin{cases} B_1 \exp(K_1 x), & x < 0, \\ B_2 \exp(-K_2 x), & x > 0, \end{cases}$$

where $cK_1 = (c^2 k_y^2 - \omega^2 \epsilon_1)^{1/2}$ and $cK_2 = (c^2 k_y^2 - \omega^2 \times \epsilon_2)^{1/2}$. Application of the jump conditions at $x = 0$ obtained from the differential equation,

$$B|_{x=0+} = B|_{x=0-},$$

$$\frac{1}{\epsilon_1} \frac{dB}{dx} \Big|_{x=0+} = \frac{1}{\epsilon_2} \frac{dB}{dx} \Big|_{x=0-},$$

leads to the dispersion relation for surface waves:

$$K_1 / \epsilon_1 + K_2 / \epsilon_2 = 0. \quad (3)$$

The well-known surface wave with frequency $\omega_p / 2^{1/2}$ is obtained in the limit $ck_y / \omega \gg 1$, when $n_1 = 0$. Since from the dispersion relation, Eq. (3), ϵ_1 and ϵ_2 must have opposite sign, one of the densities must be above critical while the other must be below. Furthermore, both densities must be greater than $n_c \cos^2 \theta$ (where $\sin \theta = ck_y / \omega$,

and n_c is the critical density at which $\omega = \omega_p$) in order that the solutions be evanescent. Thus, if n_2 is taken as the larger of the two, $n_2 \geq n_c$ and $n_c \cos^2 \theta \leq n_1 \leq n_c$. For $\nu = 0$, the relation between these densities required for the existence of a surface wave as obtained from Eq. (3) is

$$n_2 / n_c = 1 + (n_c - n_1) \sin^2 \theta / (n_1 - n_c \cos^2 \theta).$$

Curves of n_2 versus n_1 for several values of θ are shown in Fig. 1(a).

In order to obtain absorption from a surface wave, some form of dissipation must be present. The first of three possibilities is collisional absorption. If collisions are strong their effect is easily obtained from the dispersion relation Eq.

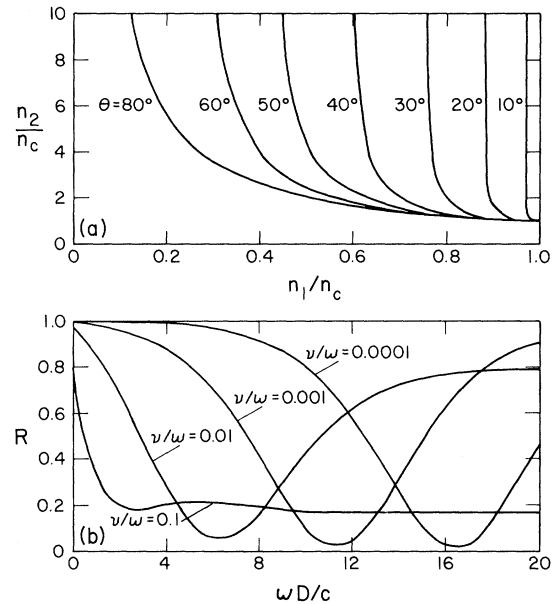


FIG. 1. (a) The plasma densities on either side of a step discontinuity in density along which a surface wave may propagate are plotted against each other for various values of θ . n_c is the critical density and $\sin \theta = ck_y / \omega$ where k_y is the wave number perpendicular to the surface normal. (b) Power reflection coefficient R as a function of D , the distance between the two jumps, for a double-step density profile. ν is the electron-ion collision frequency; $n_1 = 0.8n_c$, $n_2 = 2n_c$, and $\sin \theta = 0.5$.

(3) with $\nu \neq 0$. In the second possibility, ν may be regarded as an anomalous collision frequency describing dissipation arising from parametric decay, oscillating-two-stream, and other nonlinear absorption mechanisms whose scale lengths are small compared to typical surface-wave dimensions. A third possibility arises from the well-known pole upon which zero-electron-temperature resonant absorption is based. In any realistic plasma profile, the jump from n_1 to n_2 will occur over some length. If this length is small, surface waves still exist, but a dissipative term is obtained which is proportional to this length and which remains finite in the limit $\nu \rightarrow 0$. An analysis of this effect is contained in Ref. 4.

An idealized density profile in which surface-wave absorption occurs is the "double step" profile. Here the density rises from zero outside the plasma to the density n_1 . The density then remains constant for the distance D before it rises to the final value n_2 . The region having density n_2 then extends to infinity and the densities n_1 and n_2 are chosen to allow a surface wave to propagate on the second jump.

The large absorption in the presence of weak surface-wave damping arises as follows.⁷ When the incoming electromagnetic wave encounters the first density jump it becomes evanescent. In the absence of any further jumps in the profile it would be essentially all reflected. The energy tunnels in, however, to the second density jump. Here it resonantly excites a surface wave to an amplitude dependent on the damping seen by the surface wave. The fields from this surface wave then extend back to the first density jump. If the distance D between the two density jumps is chosen correctly, these fields interfere destructively with the reflected fields, giving negligible reflection, and hence large absorption.

This simple case can be analyzed by considering three regions and matching solutions across the two density jumps. A known incoming wave and unknown outgoing wave are assumed at $x \rightarrow -\infty$. The reflection coefficient R is the square of the magnitude of the ratio of outgoing to incoming wave amplitudes:

$$R = \left| \frac{F_- G_- + F_+ G_+ \exp(2k_1 D)}{F_+ G_- + F_- G_+ \exp(2k_1 D)} \right|^2,$$

$$F_{\pm} = i |(\omega/c) \cos \theta| \pm k_1 / \epsilon_1, \quad G_{\pm} = k_1 / \epsilon_1 \pm k_2 / \epsilon_2.$$

This reflection coefficient as a function of D is plotted for the case $n_2 = 2n_c$, $n_1 = 0.8 n_c$, and $\theta = 30^\circ$ for several values of ν in Fig. 1(b).

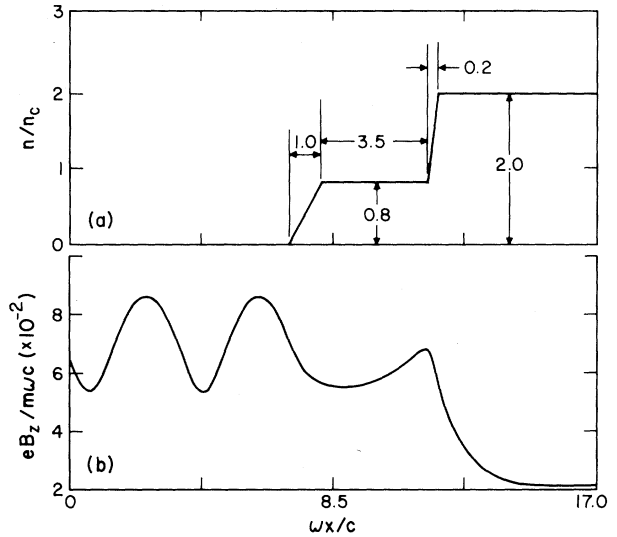


FIG. 2. (a) Ion density as a function of x used in two-dimensional simulation. The wave was launched from the left at an angle of 30° to the x axis such that $k_y = 2\pi/L_y$. The dimensions of the computational region were $L_x = 17c/\omega$ with 117 cells in x and 128 in y . Fixed ions and 64 000 electrons with $V_{th}/c = 0.0707$ were used with a time step of $0.0475\omega^{-1}$. The wave amplitude was picked to give a free-space oscillating velocity for an electron of $V_0 = 0.05c$. Electrons were bounced at the left boundary, and absorbed and reemitted with the initial thermal velocity at the right. (b) Magnitude of B_z as a function of x predicted numerically by integrating Eqs. (1) and (2), using a Debye-smoothed electron density.

In many cases of physical interest, however, the dissipation which arises from finite slopes at the steps dominates. Although an approximate analysis has been carried out for an assumed linear density rise over a distance short compared to the evanescent lengths involved, the results are barely adequate and numerical integration of Eqs. (1) and (2) is to be preferred. Absorption coefficients for a number of cases have been obtained in this way and they compare favorably with the results of computer simulation studies.

92% absorption was observed in one such computer simulation run whose results are presented below. In Fig. 2 the relevant simulation parameters are indicated along with the ion density profile used and the B -field shape predicted for that case.

In the simulation, 90% of the absorbed energy reappears as fast electrons which have been accelerated back out of the plasma into the vacuum. The large component of E_x at the critical density that accelerates these electrons is shown in Fig.

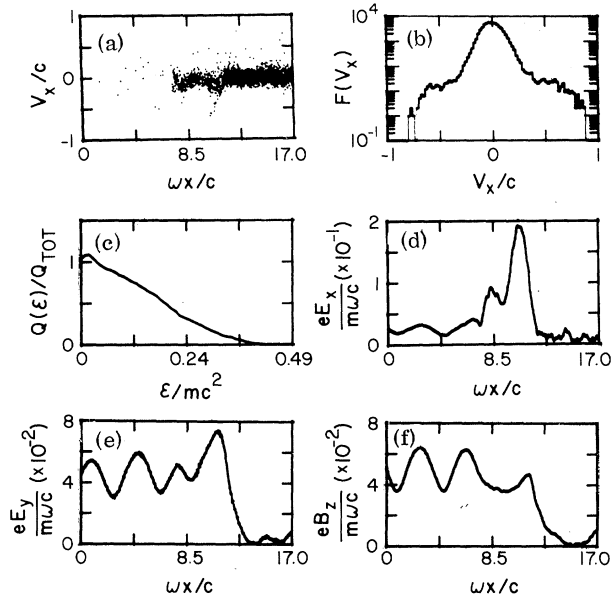


FIG. 3. Results of simulation described in Fig. 2(a). (a) Phase space at a fixed value of y . (b) x -velocity distribution function averaged over computational region. (c) Energy flow out of right boundary carried by electrons with energies greater than ϵ as a function of ϵ . (d)–(f) Electromagnetic field components as a function of position. Fields are Fourier analyzed in y and the magnitudes of the $k_y = 2\pi/L_y$ components are plotted as a function of x .

3(d). In V_x -versus- x phase space [Fig. 3(a)] the “sloshing” motion of the bulk electrons in the neighborhood of the critical density along with the acceleration of a few to very large velocities is clearly seen. The resulting velocity distribution in V_x averaged over the computational region is shown in Fig. 3(b). As the fast electrons pass back through the plasma after reflection from an electrostatic sheath at the boundary they are relatively unaffected by the fields because of their high velocities. They are then absorbed at the right boundary of the computational region, analyzed, and reemitted at the initial temperature of the plasma. The x component of the heat-flow vector per unit energy ($dQ_x/d\epsilon$) is then obtained by accumulating the net energy carried out of the computational region as a function of energy $\epsilon = \frac{1}{2}mv^2$. Integrating this quantity from a fixed value of ϵ to infinity defines $Q_x(\epsilon)$.

As can be seen in Fig. 3(c), 50% of the absorbed energy is carried out by electrons with energies in excess of 100 keV and 90% is carried by electrons having energies in excess of 30 keV. For

a half-Maxwellian in which $T_x \gg T_y \approx T_z$, 73% of the energy is carried by particles having $\epsilon \geq T_x$. Assuming the fast-electron distribution is Maxwellian and using this result, a temperature of 60 keV is obtained for the fast electrons. These energies are observed to scale roughly as the square root of the incident power density.²

Evidence that a surface wave is indeed present is seen in Fig. 3(f). At $x = 8c/\omega$ the incoming wave becomes evanescent. If no surface wave were present, i.e., if the density behind the jump were $100n_c$ instead of the $2n_c$ required for the surface-wave resonance, it would decay away to the right with, perhaps, a change in evanescent length as it goes from the low-density to high-density region. Instead the amplitude rises in the neighborhood of the density jump, and falls sharply in the high-density region because of the smaller evanescent length. The same behavior is seen in the B field as a function of position predicted by numerically integrating Eqs. (1) and (2) shown in Fig. 2(b). The predicted absorption from this calculation is 90% which also agrees quite well with the 92% absorption observed in this simulation.

We wish to thank Dr. C. W. Nielson for the use of the plasma-simulation code WAVE and Dr. D. W. Forslund for the use of his vector-Gaussian-elimination routine.

*Work performed under the auspices of the U. S. Atomic Energy Commission.

¹R. P. Godwin, Phys. Rev. Lett. **28**, 85 (1972); N. G. Denisov, Zh. Eksp. Teor. Fiz **31**, 609 (1956) [Sov. Phys. JETP **4**, 544 (1957)]; V. L. Ginzburg, *Propagation of Electromagnetic Waves in Plasmas* (Pergamon, New York, 1970), p. 260 ff; A. D. Piliya, Zh. Tekh. Fiz **36**, 818 (1966) [Sov. Phys. Tech. Phys. **11**, 609 (1966)]; A. V. Vinogradov and V. V. Pustavalov, Pis'ma Zh. Eksp. Teor. Fiz. **13**, 317 (1971) [JETP Lett. **13**, 226 (1971)]; K. G. Budden, *Radio Waves in the Ionosphere* (Cambridge Univ. Press, Cambridge, England, 1961), p. 348 ff; P. Hirsch and J. Shmoys, Radio Science **690**, 521 (1965).

²J. P. Freidberg, R. W. Mitchell, R. L. Morse, and L. I. Rudsinski, Phys. Rev. Lett. **28**, 795 (1972).

³R. B. White and F. F. Chen, Plasma Phys. **16**, 565 (1974).

⁴P. K. Kaw and J. B. McBride, Phys. Fluids **13**, 1784 (1970).

⁵A. W. Trivelpiece, *Slow Wave Propagation in Plasma Waveguides* (San Francisco Press, San Francisco, Calif., 1967); A. A. Vedenov, Usp. Fiz. Nauk **84**, 533 (1964) [Sov. Phys. Usp. **7**, 809 (1965)]; R. L. Guernsey, Phys. Fluids **12**, 1852 (1969); R. H. Ritchie, Progr. Theor. Phys. (Kyoto) **29**, 607 (1963); A. W. Trivelpiece

and R. W. Gould, *J. Appl. Phys.* **30**, 1784 (1959).

⁶D. W. Forslund, J. M. Kindel, K. Lee, and E. L. Lindman, LASL Progress Report No. LA 5542-PR, 1973 (unpublished), p. 67.

⁷E. L. Lindman, J. M. Kindel, and K. Lee, in Proceedings of the Fourth Annual Anomalous Absorption Conference, Lawrence Livermore Laboratory, 8-10 April 1974 (to be published), p. C1.

Faraday-Rotation Measurements of Megagauss Magnetic Fields in Laser-Produced Plasmas*

J. A. Stamper and B. H. Ripin

Naval Research Laboratory, Washington, D. C. 20375

(Received 24 October 1974)

Magnetic fields in the megagauss range have been observed in the laser-produced plasma near the focus of a high-power laser pulse. Faraday-rotation measurements utilizing the light of a probing beam and the specularly reflected laser light both show the presence of these large fields.

We report here the first direct observations of spontaneous megagauss magnetic fields in laser-produced plasmas. Spontaneous magnetic fields have previously been measured in laser-produced plasmas formed when a high-power laser pulse was focused onto a solid target,¹⁻³ or into a gas.⁴ The earlier measurements were made with magnetic probes at some distance from the laser focus. Although these fields, measured in the expanding plasma, were as large as a kilogauss,² theory^{2,5-7} predicts that very large fields (megagauss) exist in the focal region. The megagauss fields may be of considerable importance since they can affect the physics of laser fusion in a variety of ways.⁸⁻¹¹ The direct observation of large magnetic fields should stimulate further theoretical studies of their effect on laser fusion.

It has been recognized that measurements of magnetic fields in the focal region require optical techniques since magnetic probes cannot give reliable data closer than 3 or 4 mm from the focus.¹¹ In this Letter, we describe two independent measurements involving Faraday rotation of electromagnetic waves. One method uses a probing beam of second-harmonic light ($0.53 \mu\text{m}$) with the data recorded on film. The other method uses the light ($1.06 \mu\text{m}$) which is specularly reflected from the critical surface of the plasma and depends on measuring (with photodiodes) both components emerging from a polarizing prism. The methods are thus independent and complementary. Analysis shows that the results of both methods are consistent with magnetic fields in the megagauss range. A brief theoretical discussion is given which shows that megagauss magnetic fields in the observed direction are expected for the reported experimental conditions.

The laser system used in these studies consists of a Nd-doped, mode-locked, mode-selected, yttrium-aluminum-garnet oscillator with a Nd-doped-glass amplifier chain.¹¹ The pulse width for the studies reported here was 100 psec; pulse energy was typically 2 J. The laser beam was focused with a 3-in.-diam, $f/14$ lens producing an irradiance of about 10^{15} W/cm^2 . Targets were located in a vacuum chamber having a base pressure around 10^{-4} Torr.

The experimental arrangement for studies using a probing beam are shown in Fig. 1(a). The probing beam was obtained by splitting off part

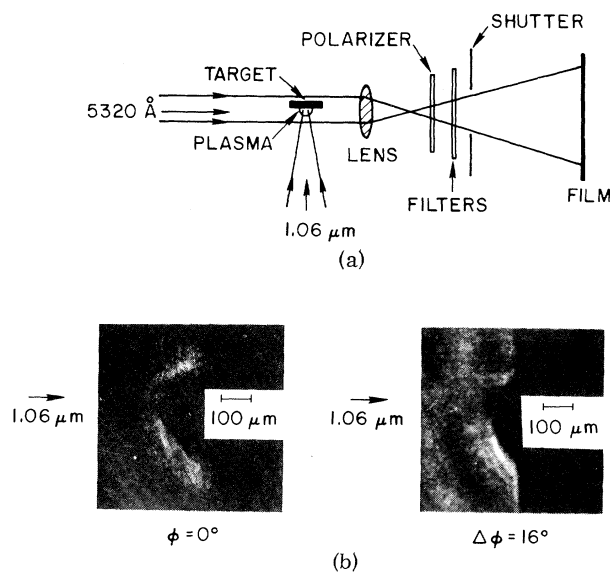


FIG. 1. Measurements of Faraday rotation of a probing beam. (a) Arrangement for detecting the rotation of polarization. (b) Sample photographs as a function of polarizing-sheet orientation.